International Journal of Heat and Mass Transfer 52 (2009) 396–406

Contents lists available at ScienceDirect

International Journal of Heat and Mass Transfer

journal homepage: www.elsevier.com/locate/ijhmt

A numerical study of heat transfer performance of oscillatory impinging jets

Buddhika N. Hewakandamby

Department of Chemical and Process Engineering, University of Sheffield, Mappin Street, Sheffield, S1 2JD, United Kingdom

ARTICLE INFO

Article history:
Received 5 June 2007
Available online 17 August 2008

Keywords:
Impinging jets
Oscillatory flow
Heat transfer
Nusselt number
Heat transfer coefficients

ABSTRACT

Enhancement of heat transfer to a planar surface by oscillating jets is presented in this work. Two jets from adjacent slots are made to oscillate with the same frequency but with a phase shift of $\pi/2$. The two nozzles are idealisation of an array of oscillating jets. A two-dimensional model is developed using finite element methods to investigate the heat transfer performance with respect to the oscillation frequency, geometric parameters and the flows with Reynolds number in the range of $0 < Re \leqslant 1200$. The computational results show that the oscillatory flow jets achieve approximately 100% improvement of heat transfer efficiency over conventional steady flow jets. It is shown that the periodic disruption of the boundary layer leads to this improvement. Further, the analysis shows the existence of a range of frequencies that are effective depending on the separation between the nozzles. The study shows that frequencies as low as 1 Hz are effective depending on the nozzle separation.

1. Introduction

Improvements to the heat transfer performance of jets impinging on a planar surface are of importance and several investigations has been reported recently [1–3]. These experimental and numerical investigations are focussed on improving heat transfer rates and minimising the variation of lateral temperature distributions by oscillating the jets. Periodic oscillations are imposed either by acoustic excitation [2,4] or mechanical pulsation [3]. Oscillations perturb the boundary layer thus influencing the local heat transfer rates. Even though impinging jets usually operate at high Reynolds numbers, applications such as cooling electronic components and the drying of thin film coatings on circuit boards could benefit from operating at low Reynolds number flow regimes. In the latter application, it is essential to keep the spatial variations of the temperature to a minimum as this could lead to non-uniformities in film thickness due to localized Marangoni stresses. This paper investigates numerically the effect of multiple jets oscillating out of phase at low Reynolds numbers ($0 < Re \leqslant 1250$).

An impinging jet has well defined regimes, namely a free jet region where the flow is developing with disappearing potential core, a stagnant region where the jet impinges on the plane, and a wall jet region [5]. A boundary layer starts to grow from the point of impingement which is also known as the stagnation point. The strong acceleration in this region keeps the boundary layer laminar [6]. For a single impinging laminar jet, it is widely known that the curve showing the local Nusselt number against the position takes a bell shape having the maximum at the stagnation point. This implies that the local heat transfer rate decreases with the growth of the boundary layer. Wall jets separate from the impingement surface some distance downstream. In the case of multiple impinging jets, the wall jets from adjacent nozzles collide forcing them to separate from the planar surface. This interaction forms a secondary stagnation point as shown in Fig. 1. Counter rotating vortices form in the secondary stagnation region [7,8] hindering the local heat transfer. As a result, the Nusselt number takes the minimum value at the secondary stagnation point. The upwash either flows out if allowed by design or interacts with the cross-flow forming complex structures depending on the geometry and the flow parameters [7].

The effect of oscillating the impinging jets at low Reynolds number regimes has been the focus of a few investigations. A numerical study of the heat transfer performance of a confined pulsed laminar impinging jet by Poh et al. [9] shows that the spatial distribution of the time averaged Nusselt numbers become Reynolds number invariant in the laminar jet regime ($100 \leqslant Re \leqslant 1000$). They demonstrated that the local Nusselt number at the wall jet separation region remains constant during the oscillation cycle. They hypothesised that the vortices formed between the wall jet and the nozzle plate decelerate the wall jets, leading to a constant Nusselt number. The single jet dynamics studied in their work suggest that the oscillation frequency has little bearing on the heat transfer rate. Mechanisms affecting the heat transfer of an externally perturbed impinging hot jet ($Re = 1000$) are numerically examined by Jiang et al. [10]. Forced oscillations are induced by introducing small perturbations to all three velocity components. This shows that the wall jet symmetry is broken, leading to fluctuations in the local heat transfer. Formation of low intensity vortices along the jet is also reported and thought to enhance the heat transfer between the jet and the ambient fluid.

E-mail address: b.n.hewakandamby@shef.ac.uk

0017-9310/$ - see front matter © 2008 Elsevier Ltd. All rights reserved.
doi:10.1016/j.ijheatmasstransfer.2008.07.004

Nomenclature

C_p	heat capacity
D	nozzle width
f	frequency
H	height to nozzle
h	local heat transfer coefficient
k	thermal conductivity
$\boldsymbol{n}$	unit normal vector to a surface
p	pressure
q	heat flux
S	nozzle separation
T	temperature
t	time
$\boldsymbol{t}$	unit tangent vector to a surface
$\boldsymbol{u}$	velocity vector
v	y component of the velocity

Greek symbols

α	heat diffusivity
μ	dynamic viscosity
ν	kinematic viscosity
ρ	density
τ	period of the oscillation
∇	differential operator

Subscripts

f	fluid phase
i	initial value
o	quantity defined on a boundary
s	surface

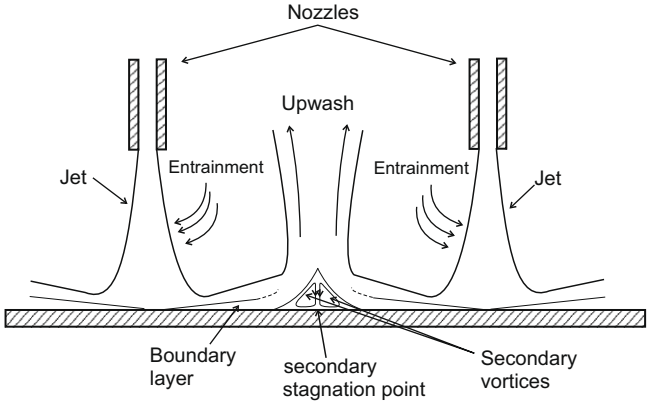

Fig. 1. Schematic diagram of multiple jet impingement.

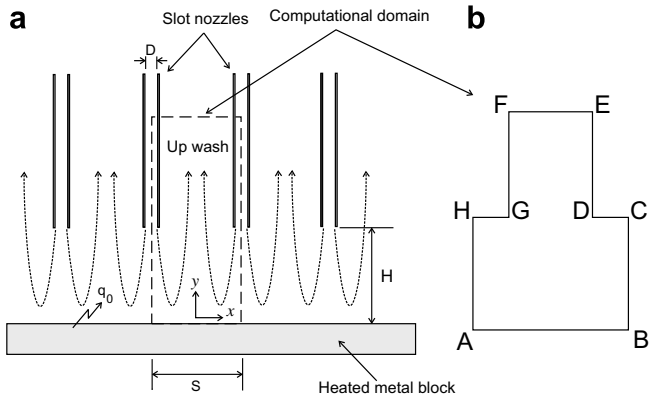

Fig. 2. Schematic diagram of the nozzle arrangement (a) and the computational domain (b) considered in numerical simulations.

In the above investigations, the effects of a single oscillating jet on heat transfer are examined. The periodic oscillations of the boundary layer result in varying local heat transfer coefficients. However,it is suggested in the present paper that the boundary layer could be disrupted to a greater extent by the use of multiple jet arrays oscillating out of phase. In an array of jets, two such nozzles form a unit that operates cooperatively. The phase difference between the jets forces the wall jets to oscillate laterally. This causes the boundary layer to be disrupted and then to reform at least once during a single flow cycle. Further, the lateral movements of the wall jets periodically oscillate the jet interaction point (or line) along the surface between the jets, destroying the symmetry. It is expected that this motion will reduce the high-temperature region that forms at the secondary stagnation point in multi-jet arrays. Considering the continuous shearing of the boundary layer and the lateral oscillation of the secondary stagnation point, it is hypothesised that heat transfer should be improved compared with steady jets of the same geometric arrangement. A numerical analysis of this hypothesis is presented below.

2. Method of analysis

As outlined Section 1, an array of slot-nozzles placed at a distance H above a constantly heated planar surface as shown in Fig. 2(a) is considered. The slot-nozzle width and the separation between the slot centres are defined as D and S, respectively. Laminar air jets ($0 < Re \leqslant 1250$) impinge on the hot surface and remove heat by thermal convection. Flow rates through the jets oscillate with a net positive flow into the domain. The frequency of the oscillation is taken to be f and the phase angle between adjacent jets is taken as $\pi/2$. The spent air is allowed to leave the domain assuming there is no nozzle plate. The heat transfer performance of the oscillatory flow unit is compared with the conventional steady flow jets for the same geometry. Further, the performance of the oscillatory flow is analysed to determine:

(1) the influence of the Reynolds number,
(2) the effect of the nozzle separation S,
(3) the impact of the frequency on heat transfer.

2.1. Governing equations

This study focuses on low Reynolds number laminar jets. The jet is characterised by the Reynolds number based on jet exit velocity U and the nozzle diameter D

$$Re = \frac{\rho U D}{\mu} \tag{1}$$

Under the laminar jet impingement, the boundary layer on the horizontal plate should grow to its maximum thickness within a few diameter lengths. Flow within the computational domain is determined by solving the Navier–Stokes equations and the continuity equation subject to appropriate boundary conditions

$$\frac{\partial \boldsymbol{u}}{\partial t} + (\boldsymbol{u}\cdot\nabla)\boldsymbol{u} = -\frac{1}{\rho_f}\nabla p + \nu\nabla^2\boldsymbol{u} \tag{2}$$

$$\nabla\cdot\boldsymbol{u} = 0 \tag{3}$$

No-slip boundary condition is assumed at AB

$$\boldsymbol{u} = 0 \tag{4}$$

As AH and BC are the boundaries along the centrelines of the two nozzles, slip-symmetry boundary condition is imposed. This requires the velocity to be normal to the boundary and the tangential forces along the boundary to vanish

$$\boldsymbol{n}\cdot\boldsymbol{u} = 0; \quad \boldsymbol{t}\cdot\left(-p\boldsymbol{I} + \mu\left[\nabla\boldsymbol{u} + \nabla\boldsymbol{u}^T\right]\right)\boldsymbol{n} = 0 \tag{5}$$

Jet exit velocities are defined normal to CD and GH boundaries. For the oscillatory flow, the velocity along the y direction is defined as follows:

$$v_o = -A_0 + A_w\sin(2\pi f t) \tag{6}$$

The amplitudes A_0 and A_w in above equation are selected such that $|A_0 - A_w| \geqslant 0$; a condition that guarantees a net positive flow into the domain. The root mean square (RMS) of the oscillatory flow velocity is used as the inlet velocity for the steady jets: i.e. the characteristic velocity $U = v_n$

$$v_n = \sqrt{\frac{1}{\tau}\int_0^\tau v_o^2\,dt} \tag{7}$$

where $\tau = 1/f$ is the period of the oscillation. Reynolds numbers up to a maximum of 1200 are evaluated using the RMS value of the velocity for both oscillating and steady jets. The upper boundary EF is open to the atmosphere. Hence the following pressure boundary condition is used

$$\left(-p\boldsymbol{I} + \mu\left[\nabla\boldsymbol{u} + \nabla\boldsymbol{u}^T\right]\right)\cdot\boldsymbol{n} = -p_0\boldsymbol{n} \tag{8}$$

The heat transfer within the flow domain is described by

$$\frac{\partial T}{\partial t} + \boldsymbol{u}\cdot\nabla T = \alpha_f\nabla^2 T \tag{9}$$

where $\alpha_f = \frac{k_f}{\rho C_p}$ is the thermal diffusivity.

A constant heat flux is assumed across the bottom boundary AB

$$-\boldsymbol{n}\cdot(-\alpha_f\nabla T) = \frac{q_0}{\rho C_p} \tag{10}$$

where $q_0 > 0$ is the inward heat flux. The temperature of the air streams at the inlets CD and GH remains constant at room temperature T_0

$$T = T_0 \tag{11}$$

Since the heat is convected out of the domain at EF, the convective heat flux boundary condition is imposed

$$[\alpha_f\nabla T]\cdot\boldsymbol{n} = 0 \tag{12}$$

There is no heat flow across BC and AH due to the geometric symmetry, therefore, the thermal insulation boundary condition is used

$$[\alpha_f\nabla T + \boldsymbol{u}T]\cdot\boldsymbol{n} = 0 \tag{13}$$

Eqs. (2)–(13) describe the fluid flow and heat transfer inside the domain. The physical properties considered in this study are given in Table 1. It is assumed that these properties remain constant over the temperature range considered. The values used to define the problem are given in Table 2.

2.2. Derived measures for comparison

The jet impingement convects heat away from the bottom surface. The heat transfer between the wall jet and the surface depends on the local heat transfer coefficient h_l. Therefore, a local Nusselt number based on h_l and slot width D is defined as

$$Nu(x,t) = -\frac{h_l D}{k_f} = -\frac{\partial T}{\partial y}\frac{D}{\Delta T} \tag{14}$$

in order to describe the convective heat transfer characteristics at the impingement plate. The Nusselt number is evaluated by computing the local surface normal temperature gradient, $\frac{\partial T}{\partial y}$, at the impingement surface and nondimensionalising using $\Delta T = (T_s - T_0)$ where T_s is the local temperature and T_0 is the temperature of the jet at the nozzle. A similar definition of the local Nusselt number has been employed in many other computational studies because the surface normal temperature gradient is readily available in a computational approach [10–12].

The Nusselt number varies with time and position. Therefore, to compare the oscillatory and non-oscillatory jets, a length averaged Nusselt number is defined

$$Nu(t) = \int_0^L \frac{1}{L}Nu(x,t)\,dx \tag{15}$$

To compare the overall effect of the oscillation over the fixed jet velocity, the average Nusselt number is computed by integrating over length and time

$$Nu_t = \int_0^{t_f}\frac{1}{t_f}Nu(t)\,dt = \int_0^{t_f}\frac{1}{t_f}\int_0^L\frac{1}{L}Nu(x,t)\,dx\,dt \tag{16}$$

The total time of cooling is given by t_f. Nu_t is used to compare the overall heat transfer rates between the steady and oscillating jets for a wide range of parameter values.

Table 1
Physical properties of air and the metal at 300 K

Property	Value
Density ρ_f (kg/m^3)	1.16
Viscosity μ_f (Pa s)	1.85×10^{-5}
Specific heat capacity C_p (kJ/kg K)	1.01
Thermal conductivity k_f (W/m K)	2.63×10^{-2}
Thermal diffusivity α_f (m^2/s)	2.25×10^{-5}

The values are taken from the tables given in [15].

Table 2
Parameter values used for the simulations

Parameter	Value
Initial temperature T_i (K)	300
Inward heat flux q_0 (W/m)	400
Inlet temperature T_0 (K)	300
Slot nozzle width D (m)	0.01

2.3. Solution methodology

In the arrangement shown in Fig. 2, two adjacent nozzles form a recurring unit (marked by the dashed lines). This repeating cell geometry is selected as the computational domain (shown in Fig. 2(b)).

A commercially available general finite element software package, COMSOL Multiphysics version 3.3b, is used to solve Eqs. (2)–(13). Lagrange quadratic rectangular elements are used to discretise the domains. Considering the need to resolve the boundary layer and the importance of computing the local surface-normal temperature gradient, a structured mesh with elements closely packed near the bottom boundary is used. Fig. 3 shows the mesh used to resolve the physical domain.

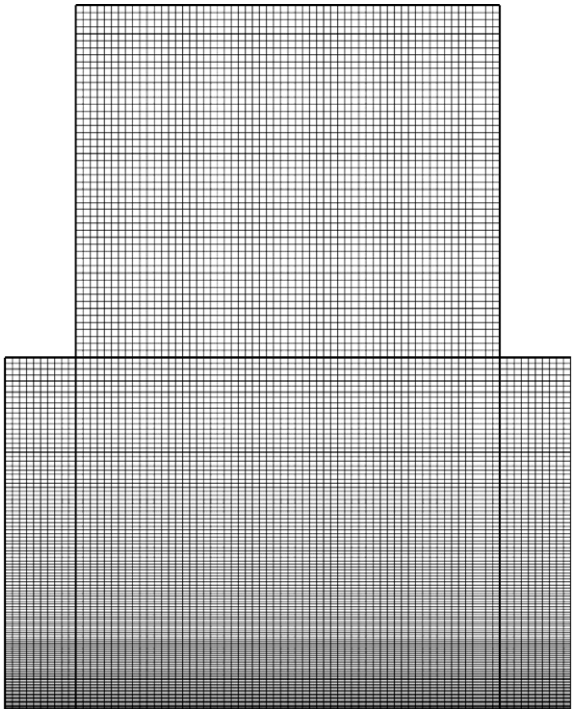

Fig. 3. Computational mesh of the physical domain. The elements grow exponentially packing a large number of nodes closer to the bottom boundary in order to capture the boundary layer development.

Grid sensitivity studies have been carried out to determine the optimum grid resolution that gives a mesh independent solution. A few structured meshes with increasing number of elements with finer packing at the hot surface are tested. Table 3 shows the details of the structured grids tested. The overall Nusselt number, as defined in Eq. (16), is computed for each mesh considered. Table 4 shows the dependence of the overall Nusselt number (Nu_t) on the discretisation for steady jets with Reynolds number 500. The nozzle separation in the test case is 4 nozzle diameters. Table 4 shows that the variation of the computed Nu_t is less than 0.03% between the meshes 2, 3 and 4. The number of degrees of freedom varies for each S/D considered. Similar tests were carried out for all the grids in deciding the discretisation. The coarsest grid that produces the error smaller than the rounding off error is selected to run the simulations.

Simulations were carried out on a dual processor workstation with 3 GHz AMD Opteron 64 bit processors with the Scientific Linux operating system. Simulation time varied from 4 to 48 h on a single processor depending on the parameter values and the number of the degrees of freedom.

Table 3
Number of elements and the corresponding number of degrees of freedom (DoF) of different meshes used to discretise the computational domain

ID	Number of elements	DoF
Mesh 1	7000	92,264
Mesh 2	9400	123,674
Mesh 3	12,600	165,554
Mesh 4	15,800	207,434

The geometry considered for the test case has a nozzle separation $S = 4D$ and nozzle to surface distance $H = 2.5D$.

Table 4
Grid dependency of the Nusselt number for steady jets with $Re = 500$

Mesh ID	Nu_t
Mesh 1	5.1582
Mesh 2	5.1129
Mesh 3	5.1110
Mesh 4	5.1113

The initial conditions imposed have an effect on the solution of any spatio-temporal simulation. In the simulations presented here, jets of air (oscillating or steady) are introduced to a quiescent environment. It takes a considerable period to dissipate the impact of the initial conditions and to develop recurring flow patterns. This phenomenon sets a lower threshold of time above which the flow becomes well established. It is observed that the time taken to develop the flow is not more than three times the retention time based on the jet exit velocity (domain area/$v_n D$) for low oscillation frequencies. For high oscillation frequencies, it takes a longer period to dissipate the initial effects. Therefore, each simulation was run well above this period to capture the true nature of the heat transfer due to the oscillations.

3. Results

3.1. Non-oscillatory flow

The performance of oscillatory jets is compared with that of steady jets. A description of the steady jets and heat transfer is included as a benchmark for the oscillatory flow. To explain the flow and heat transfer mechanisms, the nozzle configuration $S/D = 3$ and $H/D = 2.5$ with jet Reynolds number $Re = 250$ is considered. Fig. 4 shows the fully developed flow and the temperature distribution. In Fig. 4(a), the greyscale map shows the magnitude of the velocity field while the streamlines show the flow path. The jets develop with diminishing potential cores, impinge on the heated plate and form the wall jets. The wall jets from the nozzles collide and turn upward, forming a symmetric flow pattern. This flow pattern forms a secondary stagnation point, as shown in Fig. 1, entrapping a small air mass that forms weak counter rotating vortices at low Re. The secondary stagnation area accumulates heat as vortices entrain hot air from the wall jet streams into this area simultaneously with the direct heat transfer from the hot surface. Consequently, the relatively high temperature in this region leads to poor local heat transfer. This effect becomes apparent in Fig. 4(b) which shows the temperature distribution. It can be seen that a hot region has formed where the wall jets are interacting.

Fig. 5(a) shows the temperature variation along the bottom boundary (or the hot surface) for $t = 2, 4, 6, 8$ and 10 s. As explained in Section 2.3, these time-steps map the evolution of the temperature after the time taken to dissipate the effects of the initial conditions. The overlapping temperature profiles at different times suggest that the initial effects have diminished substantially within the first few time-steps and the solution has converged to a steady state. It can be seen that the temperature is minimum at the impingement points and increases to a higher value at the flow interaction stagnation point.

The variations of the Nusselt number along the hot surface are shown in Fig. 5(b). The sinusoidal variation of the Nusselt number along the surface shows that the heat transfer is at its highest where the jets impinge. Further, it shows that the Nusselt number is at its minimum where the surface temperature is at its highest. The relatively high temperature around the secondary stagnation area, as explained above, results in smaller temperature gradients lowering the local Nusselt number around the secondary stagnation point.

3.2. Oscillatory flow

The nozzle arrangement presented in Section 3.1 ($S/D = 3$ and $H/D = 2.5$) is used to show the impact of dynamical behaviour of the system. Fig. 6 shows the velocity fields and the corresponding tem-

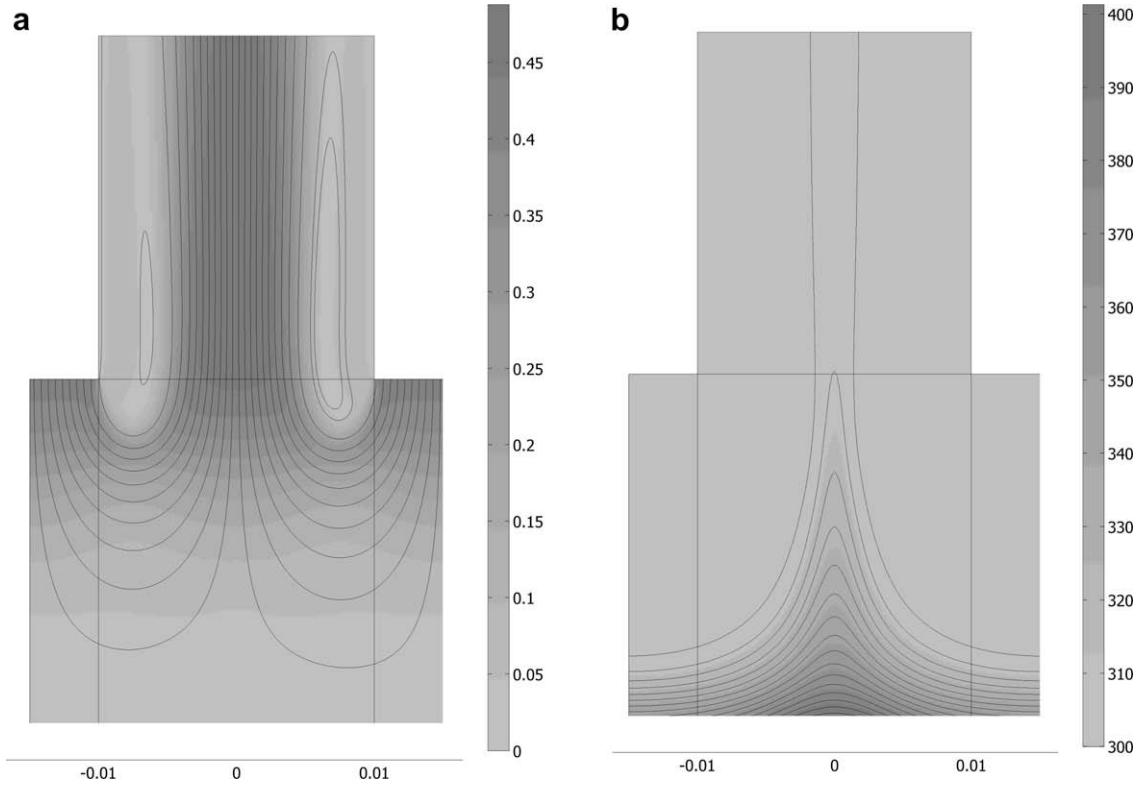

Fig. 4. Velocity field (a) and the temperature distribution (b) for non-oscillatory flow at t = 9 s. The Reynolds number is 250. $S/D = 3$ and $H/D = 2.5$.

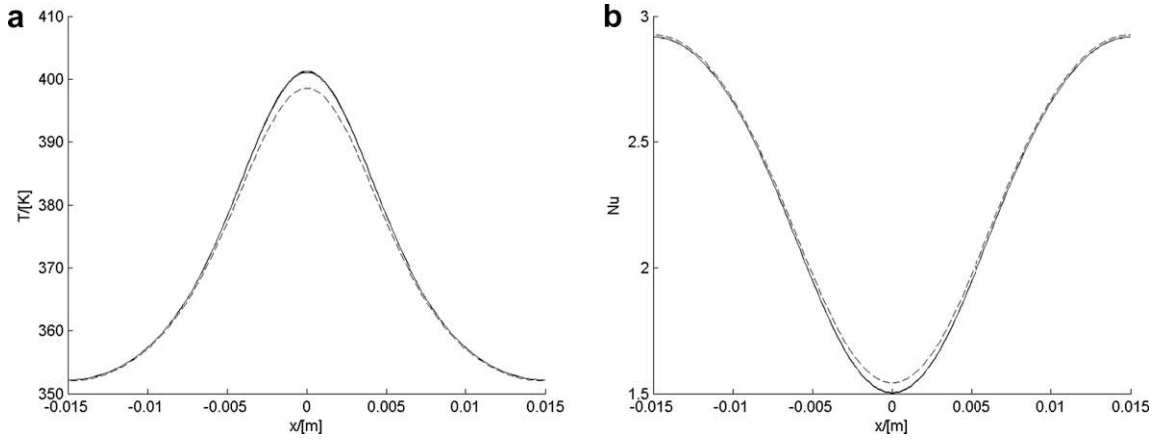

Fig. 5. Temperature (a) and the Nusselt number (b) variation along the impingement plate for non-oscillatory jets at $t = 2$, 4, 6, 8 and 10 s for the case shown in Fig. 4.

perature maps for jets oscillating at 1 Hz with $Re = 250$ between $t = 8$ and 9 s; after the cyclic flow oscillations have been established. Fig. 6(a) shows the velocity field and the streamlines at every 0.25 s interval during one oscillation. It can be seen that the oscillatory flow periodically alters the flow patterns, in contrast to steady jets, eliminating the formation of a static stagnation point. The line of interaction of the wall jets shows a dynamic behaviour moving between two adjacent nozzles with the same periodicity as of the jets.

The jet oscillations with a phase angle of $\pi/2$ between them give rise to a periodic vortex (direction of rotation is marked by the arrows in Fig. 6(a)) which switches direction with the periodicity of the jets. It can be seen that the hot air streams get mixed within the domain under the influence of these vortices.

The temperature maps corresponding to the velocity maps are given in Fig. 6(b). A relatively high-temperature region develops in the area where the wall jets interact and turn upward. This is due to the adverse effect of the small hot air mass trapped between the opposing upward turning wall jets. Unlike the case of steady jets, this air mass entrains into the bulk as the wall jet velocities are of different magnitudes. This leads to a lower temperature in the region around the wall jet interaction point. This effect could be clearly seen in Fig. 7(a) which shows the temperature distribution along the bottom surface during the same interval (between $t = 8$ and 9 s). It shows that the temperature distribution oscillates between the two nozzles with a lower temperature than that of the steady jets. Furthermore, it can be seen that a higher percentage of the surface area is at a lower temperature. Fig. 7(b) shows the corresponding local Nusselt number distribution. The wider distribution of the high $Nu(x,t)$ values shows that the heat transfer is effective at most of the surface area with higher heat transfer rates. The lowest $Nu(x,y)$ values

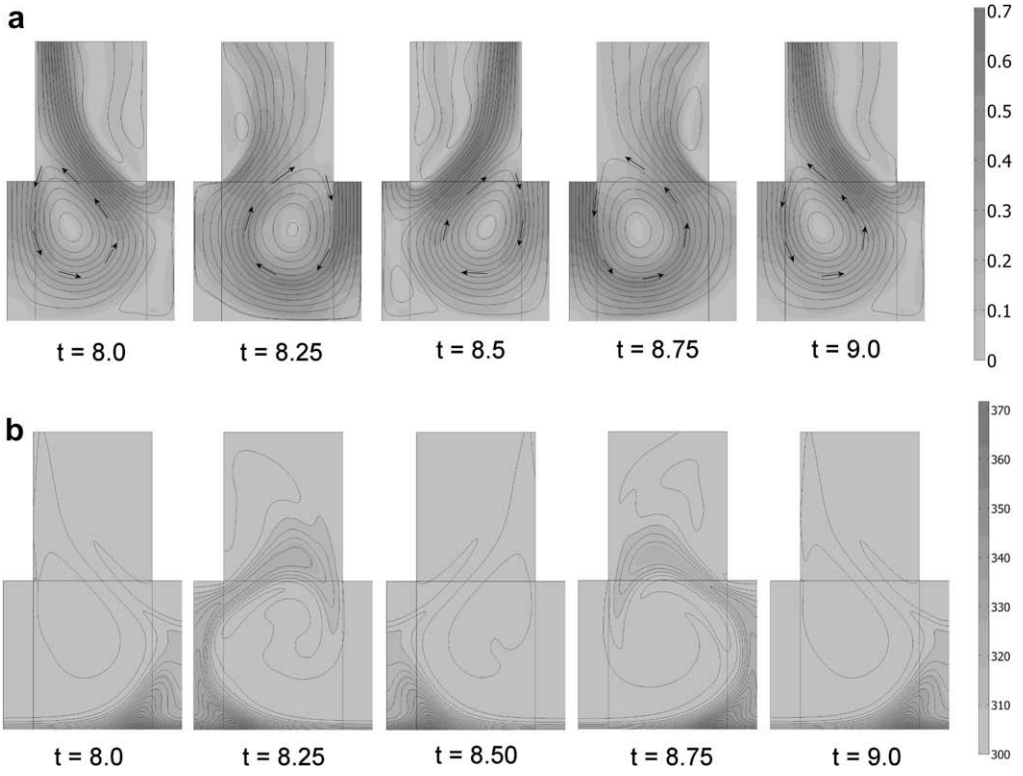

Fig. 6. Velocity (a) and temperature (b) distribution during a single cycle of oscillatory flow. The variation shown is between t = 8 and 9 s at Reynolds number 250. S/D = 3 and H/D = 2.5.

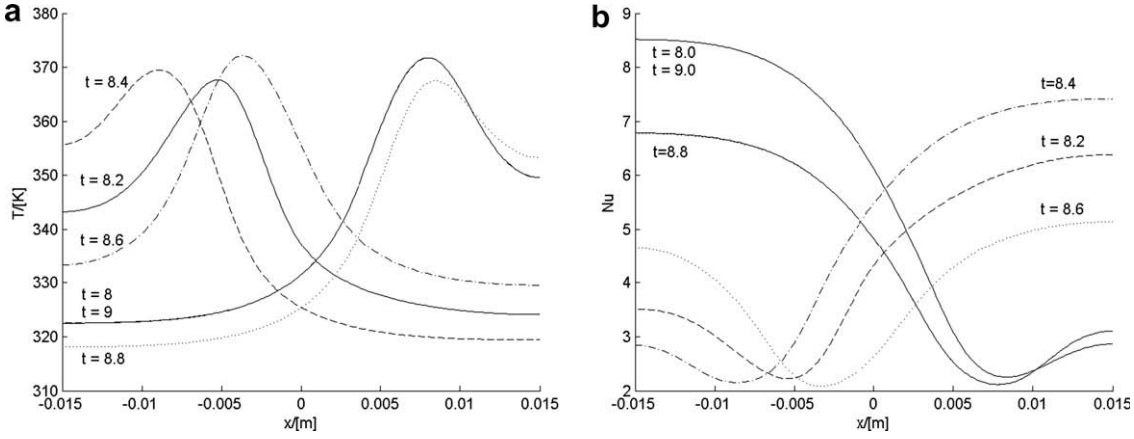

Fig. 7. Temperature (a) and the Nusselt number variation along the impingement plate during a single cycle. The Reynolds number is 250. The period is between t = 8 and 9 s.

correspond to the region where the heat transfer is poor due to wall jet interaction.

To compare the heat transfer between the steady and oscillating jets, as described in Section 2.2, the length averaged Nusselt number $Nu(t)$ is computed for each time-step. Fig. 8 shows the time evolution of $Nu(t)$ in both cases. The effects of the initial conditions are strong during the first few time-steps. $Nu(t)$ for steady jets reaches a constant value of 2.3, whereas the value for oscillatory jets varies as a periodic sine curve around a mean value of $Nu(t) = 4.4$. Despite its time periodic nature, $Nu(t)$ for oscillatory jets remains well above the values for steady jets showing better heat transfer efficiency.

3.3. Effect of Reynolds number

Heat transfer rates are generally dependent on the jet strength defined by the inlet velocity. Since the physical properties of the fluid and the characteristic length are kept constant, the Reynolds number characterises the effect of the jet velocity. Therefore, numerical experiments have been carried out to examine the effect of the Reynolds number on $Nu(t)$. Fig. 9 shows the effect of increasing Re for H/D and S/D held constant at 2.5 and 3, respectively. Fig. 9(a) shows the impact of Re on $Nu(t)$ for non-oscillatory jets. The transient behaviour of $Nu(t)$ for oscillatory jets is shown in Fig. 9(b). Reynolds numbers considered in both cases are 100, 250 and 500. $Nu(t)$ increases with increasing Re. It can be seen that oscillatory jets perform better than stationary air jets. The oscillation amplitude of $Nu(t)$ increases with the Reynolds number.

The overall performance could be captured by evaluating an overall Nusselt number Nu_t as given in Eq. (16). Nu_t values are computed by eliminating the initial effects from the simulations. Fig. 10 shows the behaviour of the overall Nusselt number Nu_t, against the Reynolds number Re for different nozzle separations. It can be seen from Fig. 10 that the heat transfer efficiency of the oscillating jets is

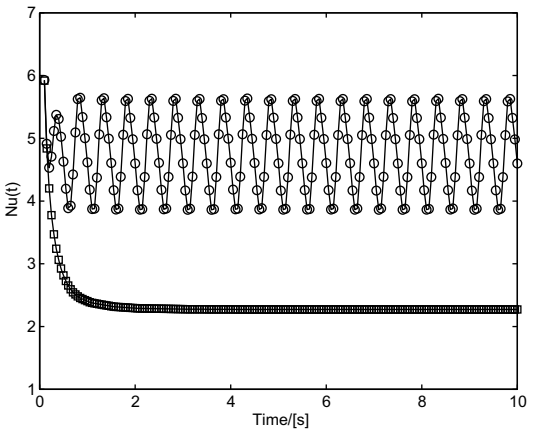

Fig. 8. Comparison between length averaged Nusselt numbers for oscillatory and non-oscillatory flows for $Re = 250$. The line with the □ markers corresponds to the steady jets while the sinusoidal line with ○ markers shows the oscillatory flow.

greatly improved over steady jets by increasing *Re* for smaller nozzle separations. For larger nozzle separations oscillatory jets are operating at the same efficiency as steady jets for the Reynolds numbers examined in this work.

3.4. Effect of nozzle separation

Nozzle separation affects the overall heat transfer rates. The overall Nusselt number as a function of the distance between the nozzles at constant Reynolds numbers is shown in Fig. 11. It can be seen that Nu_t decreases with increasing S/D for oscillatory flow with a constant *Re*. For steady jets, Nu_t reaches a maximum value around $S/D = 5$. However, it can also be seen that Nu_t for steady jets remains above the values for oscillatory flow for larger separations. Heat transfer rates for larger nozzle separations could be improved by oscillating the jets at higher *Re*.

3.5. Effect of frequency

The influence of the oscillation frequency on heat transfer is shown in Fig. 12. The jet oscillation frequency varied for the configuration $S/D = 3$ and $H/D = 2.5$ while keeping the Reynolds number constant at 250. Frequencies around 10 Hz are ineffective compared to the performance of the frequencies of the order 1 and 100 Hz. At $f = 10$ Hz, the Nusselt number achieves the lowest value, indicating poor heat transfer. However, the $Nu(t)$ achieved by oscillating the jets at 10 Hz has the same magnitude as that of the steady jet at $Re = 250$ for the same geometry. The reason for this is that the oscillation amplitude of the wall jets depends on the separation and the frequency of the jets. For $S/D = 3$, the wall jet oscillation amplitude becomes minimum around $f = 10$ Hz. As a result, a stagnation point similar to that of steady jets forms where the wall jets interact. The stagnation point vibrates around a fixed position due to the flow field fluctuations above the wall jets. Therefore, the values of $Nu(t)$ oscillate around the values closer to that of the non-oscillatory jets. This also eliminates the periodic fluctuations of $Nu(t)$. At higher frequencies of the order 100 Hz and above, the wall jets oscillate laterally with a finite amplitude. As a result, the Nusselt number regains higher values.

Another noticeable feature is the time taken before reaching quasi-steady $Nu(t)$ values when jets are oscillated at high frequencies. This is a residual effect due to the initial condition. Since the jets are oscillating rapidly, the flow alteration takes time to adapt. Once the periodic flow patterns are established, heat transfer returns to the normal behaviour.

4. Discussion

In this work, oscillating jet arrays operating cooperatively out of phase are suggested as a method of improving heat transfer. The hypothesis tested is that in such flow cells, unlike the steady jets, the boundary layer will not be fully formed. The wall jet oscillation is expected to reduce the boundary layer thickness, effectively improving the heat transfer rates. Further, it was expected that the dynamic line of interaction as opposed to a fixed position would enhance heat transfer. Our observations in the numerical experiments show the hypothesis is well supported.

As opposed to the reported work on a single oscillating jet [9], where no significant impact due to the oscillation is seen, the proposed mechanism shows a considerable improvement of heat transfer. Fig. 10 shows that the overall Nusselt number Nu_t increases with the Reynolds number at a higher rate than for the steady jets. Increments of Nu_t for the oscillatory jets over steady jets, for various nozzle separations at different Reynolds numbers are shown in Table 5. From this table, it can be seen that the jet oscillations, as suggested here, are more efficient than conventional steady jets for $S/D < 5$. However, it can be seen that the increase of *Re* improves heat transfer. Fig. 10(c) shows that the Nu_t value for the oscillating jet has noticeably improved when the Reynolds number increases to 1000 with a gradient predicting rapid improvement over steady jets. Table 5 shows that the heat transfer performance improves with higher Reynolds numbers.

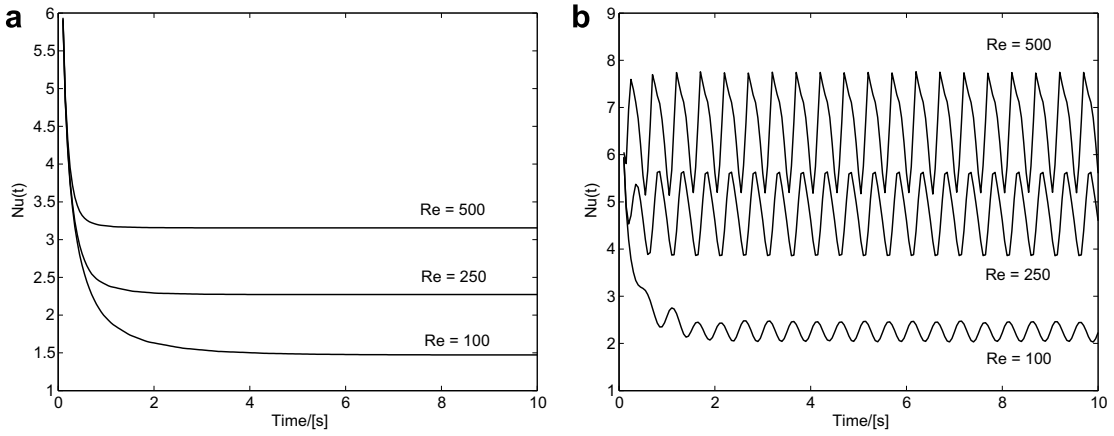

Fig. 9. Time variation of $Nu(t)$ for different Reynolds numbers. Panels (a) and (b) show the steady and oscillatory jets, respectively.

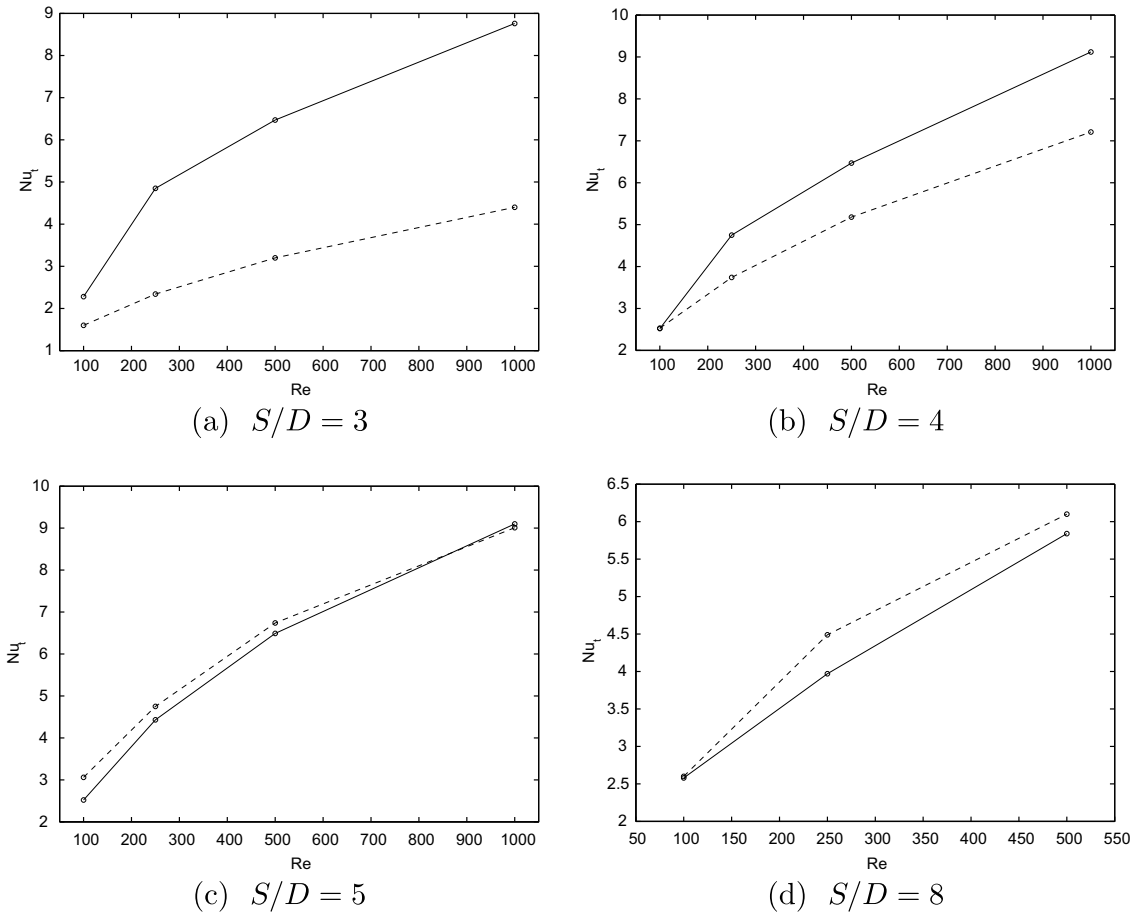

Fig. 10. Variation of Nu_t with Reynolds number for nozzle separations S/D = 3, 4, 5 and 8. The distance between the nozzle and the hot surface is kept constant at 2.5D. The continuous line corresponds to oscillatory jets and the dashed line to steady jets.

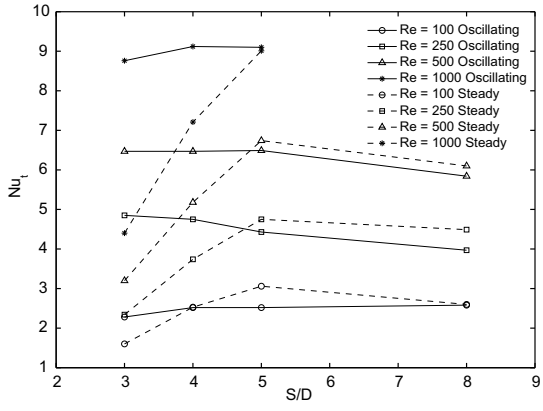

Fig. 11. The variation of Nu_t against nozzle separation ratio S/D. The nozzle height kept constant at 2.5D for all the Reynolds numbers being investigated

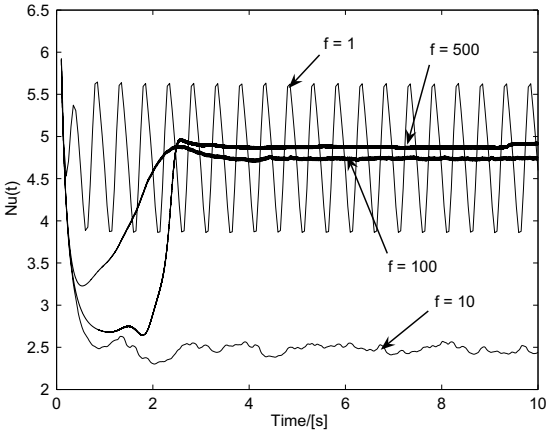

Fig. 12. $Nu(t)$ against t curves for oscillation frequencies 1, 10, 100, and 500 Hz. The nozzle separation S considered is 3D and the height H is 2.5D.

As shown in Section 3.4, the nozzle separation S/D affects the Nu_t. The higher separation between the nozzles favours the steady jets at low Reynolds numbers. This is due to the diminishing mutual influence of the jets. At large nozzle separations, the sweeping motion of the wall jets only covers a fraction of the surface area during a single oscillation. This leads to poor heat transfer characteristics. Conversely, steady jets produce wall jets with relatively constant intensity throughout the whole period giving better heat transfer efficiencies at large separations. However, the oscillating jets would operate with better heat transfer efficiencies for larger separations above a threshold Reynolds number where the wall jet interactions become dominant.

Using the above argument, one can deduce that the oscillating jets at low frequencies have no advantage over steady jets if separated beyond the distance of mutual influence. At this limit, each oscillating jet is comparable with the single jet experiments where the same conclusion is made. This argument is consistent with the numerical computations of Poh et al. [9]. The Nusselt numbers reported in [9] for a single jet with an oscillation frequency of 1 Hz at

Table 5
Comparison of overall Nusselt numbers for oscillatory (Nu_t^{Osc}) and stationary (Nu_t^{Sta}) jets

Re	Nu_t^{Sta}				Nu_t^{Osc}				$\frac{Nu_t^{Osc}-Nu_t^{Sta}}{Nu_t^{Sta}}$			
	$S/D = 3$	$S/D = 4$	$S/D = 5$	$S/D = 8$	$S/D = 3$	$S/D = 4$	$S/D = 5$	$S/D = 8$	$S/D = 3$	$S/D = 4$	$S/D = 5$	$S/D = 8$
100	1.60	2.53	3.06	2.60	2.28	2.52	2.52	2.58	0.44	−0.0039	−0.18	−0.01
250	2.34	3.74	4.75	4.49	4.84	4.75	4.43	3.97	1.07	0.27	−0.07	−0.12
500	3.20	5.18	6.74	6.09	6.47	6.17	6.49	5.84	1.02	0.28	−0.04	−0.04
1000	4.39	7.21	9.01	–	8.76	9.27	9.10	–	0.99	0.29	0.01	–

The negative sign states that the oscillatory flow is less effective than the steady flow.

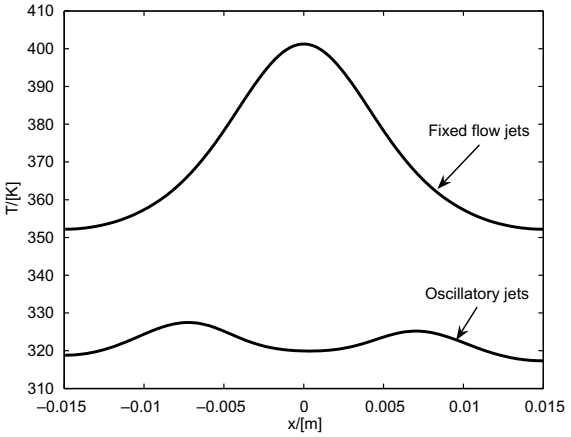

Fig. 13. Time averaged temperature profile over the surface for oscillatory and fixed flow jets between $t = 8$ and 9 s. The nozzle separation S considered is $3D$ and the height H is $2.5D$. The Reynolds number is 250.

$Re = 500$ approximately matches the Nu_t for $S/D = 8$ computation reported in this paper.

Fig. 10(c) shows the existence of a threshold value of Re for $S/D = 5$ at which the oscillation becomes more effective than conventional steady jets. Beyond this threshold value of the Reynolds number,the oscillatory jets become more effective than the steady jets. Consequently, as Fig. 12 suggests, increasing the frequency increases the heat transfer rates. Therefore, higher heat transfer rates could be achieved by optimizing the separation and the frequency. However, the results suggest that effectiveness of frequency depends on the nozzle separation. This, in turn, becomes an operational and design concern. Therefore, the appropriate frequency for the selected nozzle separation has to be determined by careful investigation.

It has been observed that the surface temperature profiles shown in Fig. 9 for oscillatory jets have lower temperatures than the equivalent steady flow. Time averaged temperature profiles for a period of oscillation in both cases are shown in Fig. 13. The temperature profile for fixed jets has a maximum at the centre of

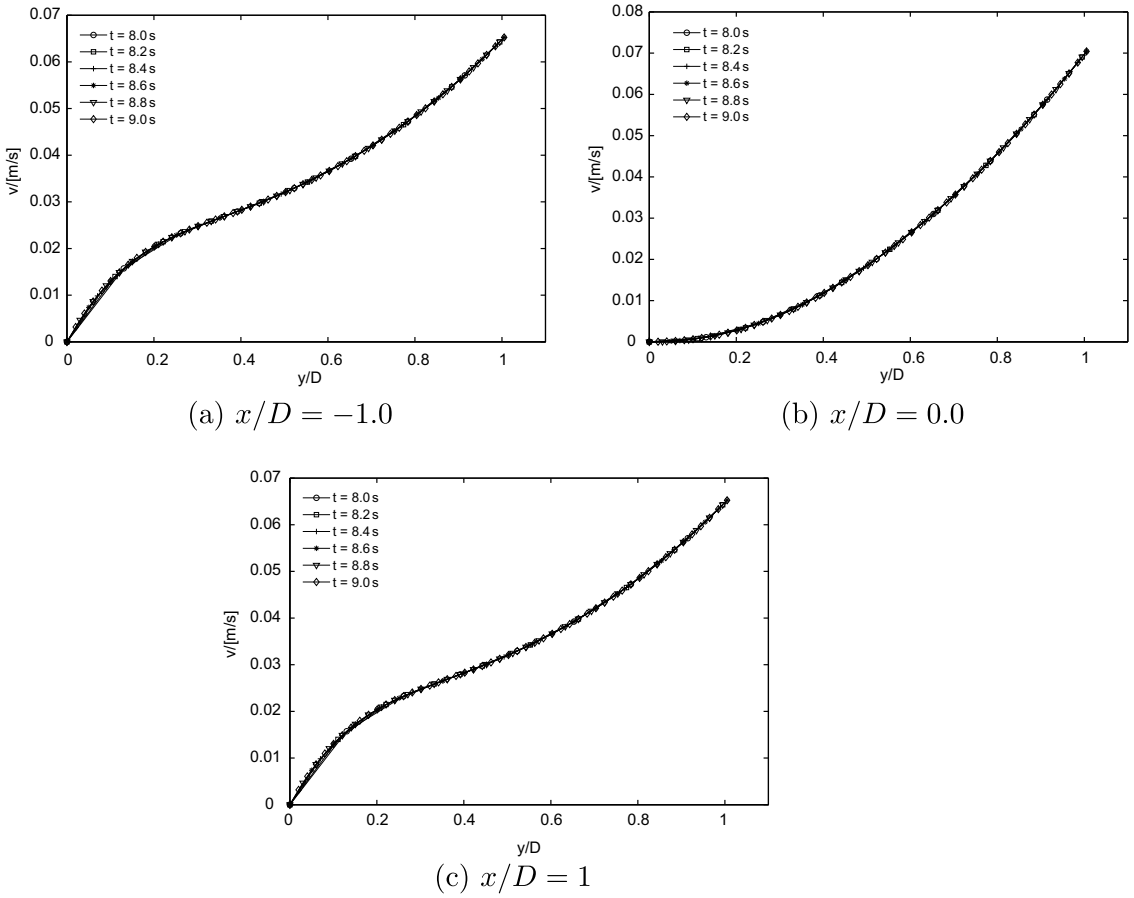

Fig. 14. Velocity profiles along lines normal to the bottom boundary at specified locations for steady jets with the parameter settings $S/D = 3$, $H/D = 2.5$ and $Re = 250$. $x/D = 0.0$ marks the centreline of the domain.

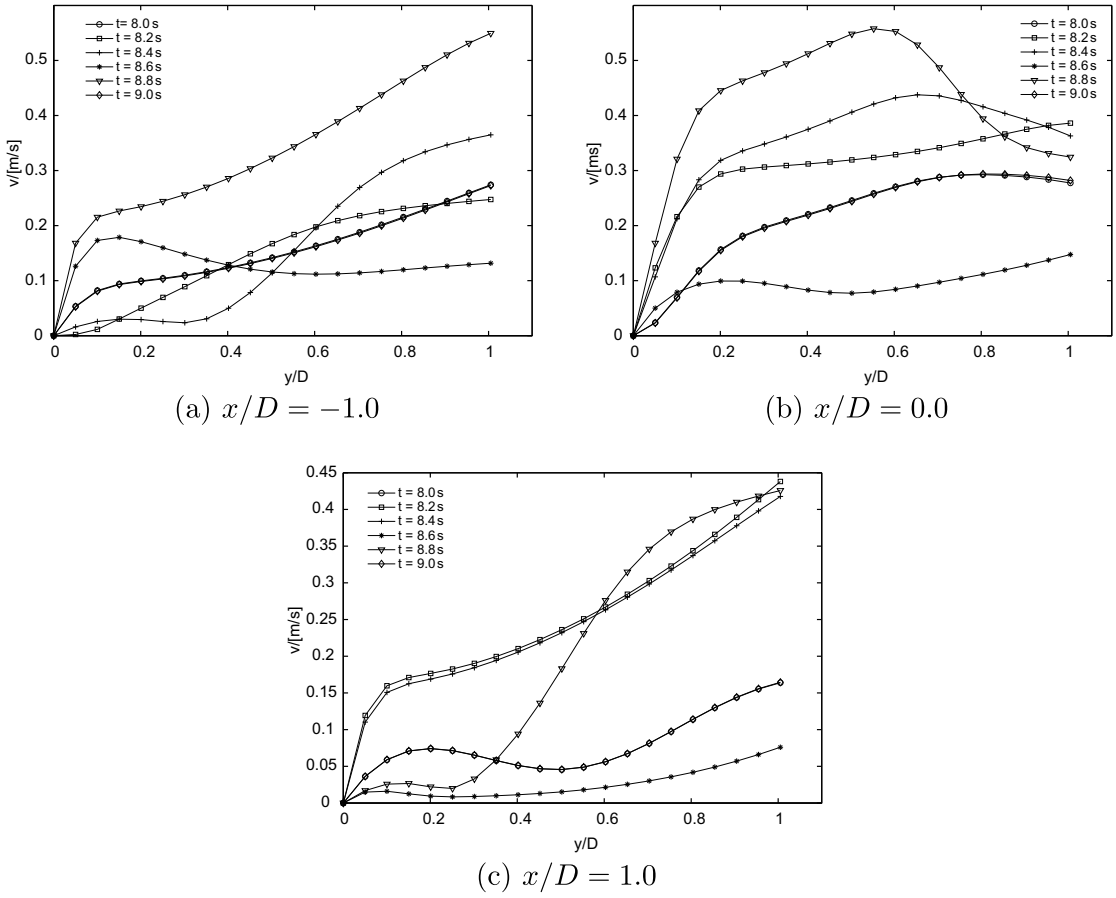

Fig. 15. Velocity profiles along lines normal to the bottom boundary at the same locations as in Fig. 14 locations for oscillating jets. Each plot shows the time variation of the velocity magnitude.

the domain where the upward turn of the flow takes place. For oscillating jets, the temperature profile contains two peaks. Unlike the case of steady jets, these local maxima occur between the centre and the nozzles. The difference between the maximum and the minimum temperatures ($T_{max} - T_{min}$) is smaller in the oscillating jets compared to steady impinging jets. For the steady jets with $S/D = 3$ and $H/D = 2.5$ at $Re = 250$, the temperature difference $T_{max} - T_{min} = 47$ K whereas for same geometric parameters, $T_{max} - T_{min} = 10$ K for the oscillating jets. This shows that the oscillating flow keeps the cooling surface at a relatively low temperature with minimum local variations. This feature is beneficial to many industrial applications where the material subjected to cooling is sensitive to residual stresses.

The mechanism leading to higher heat transfer rates and low surface temperatures is considered to be the periodic disruption of the boundary layer. Fig. 14 shows the velocity magnitudes in the y direction (normal to the hot surface) up to one diameter length, for the steady jets at regular distances along the surface for $S/D = 3$, $H/D = 2.5$ and $Re = 250$. Each figure contains the velocity profiles for five time-steps between $t = 8$ and 9 s. The velocity profiles overlap for different time-steps, showing that the velocity profile closer to the bottom remains constant during that period. This indicates that the boundary layer is formed and maintains a constant thickness at each spatial point. As a result, the thermal boundary layer remains undisturbed, imposing a constraint on the heat transfer rate. It is this regular, time-independent nature of the boundary layer that is targeted by the mechanism suggested in this paper.

Fig. 15 shows the velocity profiles up to one nozzle diameter length D along the lines normal to the bottom boundary at the same locations shown on Fig. 14. It shows that during a period of oscillation, the velocity profiles closer to the boundary vary with time, indicating that the boundary layer thicknesses also varies with time. This shows that by oscillating the adjacent jets with a phase shift of $\pi/2$, both thermal and flow boundary layers are constantly disturbed to achieve a better heat transfer performance.

The oscillations of preferred frequency could be achieved in many ways. Pneumatic and electrically controlled (solenoid) valves can be used to generate the pulsating flow. The use of a spinning circular chamber with openings that generate smooth sinusoidal oscillations are also reported [3]. There is a class of valves called fluidic oscillators operating on the principle of Coanda effect [13,14]. Such valves have no moving parts and could be integrated into existing systems to generate oscillatory flows.

5. Conclusions

The numerical studies presented here on two cooperatively oscillating slot jets with phase angle $\pi/2$ between them, show that the heat transfer could be improved greatly compared to the use of conventional steady jets. A hypothesis for the mechanisms for heat transfer enhancement is proposed with three central features: (i) the flow boundary layer thickness is minimized on average, (ii) the thermal boundary layer is disrupted and reformed periodically, and (iii) the stagnation points are no longer fixed but oscillate. This mechanistic hypothesis is well supported by the detailed study. The analysis shows that the overall Nusselt number approximately doubles for certain nozzle separations (see Table 5) when the jets are oscillated, indicating that the local heat transfer coefficient doubles with all other conditions held constant.

The heat transfer is affected by the frequency f, the separation S/D and the flow rate. Increasing the separation leads to poor heat transfer which could be improved by increasing the Reynolds number (i.e. the flow rate). It has been deduced that for any separation there will be a threshold Re value beyond which the oscillatory flow becomes more effective than the conventional approach. For a given separation, there is a range of frequencies where the heat transfer would not be improved. Oscillations outside this window of frequencies improve the heat transfer dramatically.

The time averaged temperature profile shows that the cooling surface would be at a lower temperature than that of the conventional non-oscillatory jets. Furthermore, the spatial variation of the temperature is smaller leading to homogeneous cooling; an important requirement in some applications, such as cracking due to residual stresses.

Acknowledgements

The author thank Professors William B. Zimmerman and Vaclav Tésar for very informative discussions on the subject matter. The author also thank Dr. Brian O'Sullivan, Dr. Laurent F. Jeanmeure and Dr. Martin J. Pitt for the support with the manuscript. Support from EPSRC Grant No. GR/S84347/01 is also acknowledged.

References

[1] T. Liu, J.P. Sullivan, Heat transfer and flow structures in and excited circular impinging jet, Int. J. Heat Mass Transfer 39 (17) (1996) 3695–3706.
[2] S.D. Hwang, H.H. Cho, Effects of acoustic excitation positions on heat transfer and flow in axisymmetric impinging jet: main jet excitation and shear layer excitation, Int J. Heat Fluid Flow 24 (2003) 199–209.
[3] H.M. Hofmann, D.L. Movileanu, M. Kind, H. Martin, Influence of a pulsation on heat transfer and flow structure in submerged impinging jets, Int. J. Heat Mass Transfer 50 (2007) 3638–3648.
[4] C. Gau, W.Y. Shen, C.H. Shen, Impingement cooling flow and heat transfer under acoustic excitations, J. Heat Transfer Trans. ASME 119 (4) (1997) 810–817.
[5] R. Viskanta, Heat transfer to impinging isothermal gas and flame jets, Exp. Therm. Fluid Sci. 6 (1993) 111–134.
[6] H. Martin, Heat and mass transfer between impinging gas jets and solid surface, Adv. Heat Transfer 13 (1977) 1–60.
[7] M. Can, Experimental optimization of air jets impinging on a continuously moving flat plate, Heat Mass Transfer 39 (2003) 509–517.
[8] S. Chander, A. Ray, Heat transfer characteristics of three interacting methane/air flame jets impinging on a flat surface, Int. J. Heat Mass Transfer 50 (2007) 640–653.
[9] H.J. Poh, K. Kumar, A.S. Mujumdar, Heat transfer from a pulsed laminar impinging jet, Int. Commun. Heat Mass Transfer 32 (10) (2005) 1317–1324.
[10] X. Jiang, H. Zhao, K.H. Luo, Direct computation of perturbed impinging hot jets, Comput. Fluids 36 (2) (2007) 259–272.
[11] M. Angioletti, E. Nino, G. Ruocco, CFD turbulent modelling of jet impingement and its validation by particle image velocimetry and mass transfer measurements, Int J. Heat Mass Transfer 46 (2003) 1703–1713.
[12] T. Cziesla, G. Biswas, H. Chattopadhyay, N.K. Mitra, Large-eddy simulation of flow and heat transfer in an impinging slot jet, Int J. Heat Fluid Flow 22 (2001) 500–508.
[13] V. Tésar, C.H. Hung, W.B. Zimmerman, No-moving-part hybrid-synthetic jet actuator, Sensors Actuators 125 (2) (2006) 159–169.
[14] Z. Travnicek, T. Vit, V. Tésar, Hybrid synthetic jets as the nonzero-net-mass-flux synthetic jets, Phys. Fluids 18 (8) (2006) (Art. No. 081701).
[15] F.P. Incropera, D.P. DeWitt, Fundamentals of Heat and Mass Transfer, fifth ed., Wiley, New York, 2002.